CSCanada
Energy Science and Technology
Vol. 4, No. 1, 2012, pp. 41-54
DOI:10.3968/j.est.1923847920120401.332

ISSN 1923-8460[PRINT]
ISSN 1923-8479[ONLINE]
www.cscanada.net
www.cscanada.org

A Global Kinetic Mechanism for the Prediction of Hg Oxidation by a Chlorine Species

Hans Agarwal[a]; Carlos E. Romero[b]; Fernando Hernandez Rosales[c],*; Crisanto Mendoza-Covarrubias[d]

[a]Foster Wheeler North America Corp., 53 Frontage Road, PO Box 9000, Hampton, NJ 08827, U.S.A.
[b]Energy Research Center, Lehigh University, Bethlehem, PA 18015, U.S.A.
[c]Centro de Ingenieria y Desarrollo Industrial, Santiago de Querétaro. Qro. 76130 México.
[d]Faculty of Mechanical Engineering, Universidad Michoacana de San Nicolás de Hidalgo, Santiago Tapia 403, Col. Centro, CP 58000; Morelia Michoacán, México.
*Corresponding author

Funding for this experimental work was provided by Foster Wheeler North America Corp.

Received 20 June 2012; accepted 10 August 2012

Abstract

This paper presents a global kinetic model developed from laboratory test results. The model consists of five global reactions -- two reversible and three irreversible. The reaction constants for the Arrhenius expression formulation were determined from a set of 35 experiments involving a variety of flue gas compositions that include bulk gases (N_2, CO_2 and O_2) and trace gases (NO, SO_2, Hg, Cl_2); at a range of temperatures (from 540°C to 166°C) and a variety of residence times (between 2.7 and 3.3 seconds). The values obtained for the reaction constants were further used to predict experimental data from eleven published mercury data sources. The predicted values corresponded very well compared to the observed published data.

Key words: Kinetics model; Mercury emission; Homogeneous mercury oxidation

Agarwal, H., Romero, C.E., Rosales, F.H., & Mendoza-Covarrubias, C. (2012). A Global Kinetic Mechanism for the Prediction of Hg Oxidation by a Chlorine Species. *Energy Science and Technology*, *4*(1),41-54. Available from: URL: http://www.cscanada.net/index.php/est/article/view/10.3968/j.est.1923847920120401.332
DOI: http://dx.doi.org/10.3968/j.est.1923847920120401.332

INTRODUCTION

The U.S. Environmental Protection Agency (EPA) submitted a mercury (Hg) study report to the U.S. Congress in 1997 stating that of the 158 tons of Hg released into the environment, 48 tons were derived from coal fired combustion sources (Brown, Hargis, Smith, & O'Dowd, 1999). A federal rule was issued on March 15, 2005 by EPA to permanently cap and reduce Hg emissions from coal fired power plants. Upon complete implementation, Hg emissions will be reduced by approximately 70 percent by 2018. As a consequence, a good understanding of the processes that affect the fate of Hg in coal fired boilers is important for its control.

Mercury emissions from coal fired boilers are highly dependent on Hg speciation. Mercury in the power plant flue gas stream is typically emitted in three forms: elemental mercury (Hg^0), oxidized mercury (Hg^{2+}) and particulate bound mercury (Hg^P). Hg^P is typically trapped by ash collection devices such as electrostatic precipitators (ESP) or bag houses. Hg^0 is difficult to capture since it is relatively inert, volatile at high temperatures and insoluble in water. In contrast, Hg^{2+} is very water soluble and can adsorb onto particulate matter or on metal surfaces within the power plant. Due to the differences in the physical and chemical properties of Hg^0 and Hg^{2+}, the removal of Hg is facilitated when Hg^0 is converted to its oxidized form in the gas phase. It is accepted that gas phase oxidation of Hg occurs primarily through a Cl atom recycle process, with Cl and Cl_2 both playing an important role. Other species in the flue gas, such as NO and SO_2, also affect Hg^0 oxidation under the typical conditions at the boiler back-end.

The impact of various flue gas components on the oxidation of Hg^0 has been extensively studied and attempts have been made to develop a corresponding predictive model. The following sections briefly outline experimental results and modeling efforts from prior publications. More details are given in a prior publication (Agarwal, Romero & Stenger, 2007).

1. HOMOGENEOUS MERCURY OXIDATION: EXPERIMENTAL WORK

Laudal *et al.* performed bench scale experiments to determine the effect of various flue gas components on Hg oxidation (Brown, Laudal & Nott, 2000). The bulk gas stream was heated in a Teflon-lined unit and consisted of 4 percent O_2, 15 percent CO_2, 10 percent H_2O, 20 μg/m^3 elemental Hg and a balance of N_2. The residence time was approximately one second at a constant temperature of 175°C. The Ontario Hydro Method (OHM) was used to measure Hg concentrations. They found that Cl_2 oxidizes Hg^0 effectively. However, the presence of SO_2 in the gas stream inhibited the oxidation process by Cl_2. Additional experiments by Laudal *et al.* showed that SO_2, HCl and NO_x independently did not have an effect on Hg^0 oxidation.

Norton *et al.* performed similar work as Laudal *et al.*, where the impact of NO and NO_2 was studied in greater detail (Brown *et al.*, 2002). The gas stream was heated in a stainless steel unit, and consisted of 6 percent O_2, 12 percent CO_2, 12 μg/m^3 elemental Hg and a balance of N_2. The residence time was approximately one second at a constant temperature of 180°C. The OHM was also used to measure Hg concentrations. Most experiments were performed in the presence of fly ash, which resulted in a more complicated Hg oxidation system. From the experiments that did not involve fly ash, they concluded HCl had a minor effect on Hg oxidation at this temperature. They also noted that SO_2 and NO seemed to inhibit Hg oxidation.

Ghorishi studied the effects of temperature on Hg oxidation by HCl (Ghorishi, 1998). The gas stream consisted of 5 percent CO_2, 2 percent O_2, 40 μg/m^3 elemental Hg, and a balance of N_2. The gas stream was heated in a quartz reactor. The oxidative effect of HCl on Hg^0 was studied at 515, 634 and 754 °C. The respective residence times were approximately 1.22, 1.0, and 0.97 seconds. An online Hg analyzer (Buck 400a) was used for Hg measurements. Results showed an increased level of Hg oxidation at higher HCl concentrations. In addition, at higher temperatures, the same amount of HCl resulted in a higher percent Hg oxidation, showing that HCl is a more effective oxidizing agent at higher temperatures.

Kilgroe *et al.* reported the inhibitory effect of H_2O and SO_2 on the oxidation of Hg by HCl (Kilgroe, 2001). The gas blend and experimental setup was identical to that used by Ghorishi, except temperature was maintained at 754 °C, with a residence time of 0.97 seconds. Increasing the HCl concentration resulted in an increase in Hg oxidation. In a second experiment, the addition of H_2O reduced Hg oxidation. Further addition of SO_2 in a third experiment resulted in an even further drop in Hg oxidation. They concluded that H_2O and SO_2 have inhibitory effects on the oxidation of Hg by HCl at high temperatures.

Mamani-Paco and Helble investigated the effect of HCl and Cl_2 on the oxidation of elemental Hg (Helble & Mamani-Paco, 2000). The gas blend consisted of 50 μg/m^3 elemental Hg, 26 percent of H_2O, 13 percent CO_2 and a balance of N_2, and was heated in a quartz tube to 1080°C. The residence time was varied from 1.4 to 6.2 seconds. The EPA Method 29 and a cold vapor atomic adsorption (CVAA) measuring technique were used to measure Hg concentrations. They found that HCl was less effective than Cl_2 in oxidizing Hg^0. They also claimed that the reaction between Hg and Cl_2 does not proceed below 530 °C.

Qiu *et al.* reported the effect of O_2 and SO_2 on the oxidation of Hg by Cl_2 (Helble, Qiu & Sterling, 2003). The gas blend and experimental setup was identical to that used by Mamani-Paco and Helble. The O_2 concentration in the gas stream was varied between 0.6 percent and 2.8 percent while the concentration of SO_2 in the gas stream was varied between 0 and 500 ppm_v. Increasing O_2 concentrations at a fixed SO_2 concentration resulted in a lower percent of Hg oxidized. Increasing SO_2 concentrations resulted in a further decrease in the percent of Hg oxidized. They concluded that Hg oxidation is inhibited by SO_2.

Fry *et al.* investigated the effects of Cl_2 on Hg oxidation at two quench rates (Cauch, Fry, Lighty, Senior & Silcox, 2005). Natural gas was burnt in a quartz tube and the gas composition consisted of 25 μg/m^3 Hg^0, 18.1 percent H_2O, 3.3 percent O_2, 58 ppm_v NO, 48 ppm_v CO and a balance of N_2. Mercury concentrations were measured by a Tekran 2537A Hg vapor analyzer. The concentration of Cl_2 used ranged from 0 to 300 ppm_v. The authors assumed that at their initial temperature of 1130 °C, molecular chlorine dissociated to chlorine radicals or HCl, resulting in a corresponding equivalent HCl concentration of 0 to 600 ppm_v. They concluded that an increase in the concentration of chlorine species resulted in an increase in the percent Hg oxidized. The high quench rate resulted in a higher percent of Hg oxidized at a faster rate. The lower quench rate resulted in a lower percent Hg oxidized at a slower rate.

Hall *et al.* studied the effect of temperature on Hg oxidation by HCl (Hall, Lindqvist & Schager, 1991). The gas stream was heated in a stainless steel duct and consisted of 10 percent O_2, 150 μg/m^3 of elemental Hg, and a balance of N_2. The temperatures ranged between 300 and 900 °C. Mercury concentrations were measured using a CVAA spectroscopic method. They concluded that at a fixed HCl concentration, a higher percent of Hg oxidation was observed at higher temperatures. Higher concentrations of HCl resulted in higher Hg oxidation. The effect of Cl_2 on Hg oxidation in an identical gas stream was also studied, where 12.5 to 150 ppm_v of Cl_2 was added at 500 °C. Results showed that higher Cl_2 concentrations resulted in higher Hg oxidation.

Sliger *et al.* performed similar experimental work as Hall *et al.*, (Kramlich, Marinov & Sliger, 2000) and (Sliger, 2001). The gas stream was heated in a furnace lined with refractory material and consisted of 7.43 percent O_2, 6.15 percent CO_2, 12.3 percent H_2O, 25 ppm_v NO_x, between 53 and 137 μg/m^3 of Hg^0 and the balance of N_2. The gas temperature ranged from 922 to 1071 °C. A simplified EPA Method 29 was used to measure mercury concentrations. The data showed that HCl promoted Hg oxidation but increasing the HCl concentration did not consistently increase oxidation. A second experiment varied the concentration of H_2O from 0 mole percent to 14 mole percent, at two HCl levels (39 ppm_v and 274 ppm_v). This experiment was done in a quartz reactor. The data showed that higher H_2O concentrations led to lower Hg oxidation.

Widmer *et al.* investigated the effect of temperature and HCl concentration on Hg oxidation in a simulated municipal waste gas stream, which contained high concentrations of elemental Hg (Cole, Gaspar, Seeker & Widmer, 1998). The gas stream was heated in a quartz reactor, and consisted of 10 percent O_2, 10 percent CO_2, 8 percent H_2O, 3700 μg/m^3 elemental Hg and the balance was N_2. The temperature of the gas ranged between 423 and 876°C. The EPA Method 29 was used to measure mercury concentration. They found higher temperatures resulted in higher percent Hg oxidation. As expected, higher concentrations of HCl resulted in a higher percent Hg oxidation.

Agarwal *et al.* showed the effects of various flue gas components on Hg oxidation by Cl_2 (Agarwal, Fan, Stenger & Wu, 2006). The gas stream was heated to a maximum temperature of 540 °C in a stainless steel pipe. The residence time of the gas was 1.8 seconds. The major gas components were added systematically to get a final gas composition of 70 percent N_2, 3.5 percent O_2, 13.5 percent CO_2, 13 percent H_2O, 370 ppm_v SO_2, 170 ppm_v NO, 300 ppm_v CO and 10 μg/m^3 elemental Hg. The results showed that SO_2 and H_2O inhibited Hg oxidation by Cl_2. The results also showed that higher concentrations of Cl_2 resulted in a higher percent Hg oxidation. A separate work done showed the effects of temperature on Hg oxidation by Cl_2. Using an identical setup, the gas blend consisted of either 100 percent N_2 or 87.1 percent N_2 and 12.9 percent H_2O. As temperature was increased, Cl_2 became less effective in oxidizing Hg. It was also found that H_2O inhibits the oxidation of Hg by Cl_2.

2. HOMOGENEOUS MERCURY OXIDATION: PREDICTIVE MODELING

In order to better understand the homogeneous reaction mechanism, a global predictive model needs to be developed. Several researchers have published gas phase predictive models typically by using the software Chemkin®. Examples of such a model use over 100 reactions and more than 30 reactive species (Xu, 2003) and (Lu, 2008). While the models attempt to predict the concentrations of radicals in a gas stream, to date there is no technology is available to experimentally confirm these values and offer a comparison. Additionally, the use of large numbers of reactions and reactive species make the model bulky and difficult to use. Each reaction is defined by the Arrhenius equation (discussed later) and the corresponding constants are at times empirically calculated thermodynamically. The two main constants are the pre-exponential factor (A) and the activation energy (E). In some cases, the constants end up having negative value.

Sliger *et al.* published a model that was able to predict half of their experimental data accurately (Sliger, 2001). Several activation energy values in key reactions were negative. Widmer *et al.* used a similar approach where a system of eight reactions was used to predict the interaction of elemental Hg with a chlorine species (Cole, West & Widmer, 2000). However, the activation energy of a key initial reaction was a negative value. While the model seemed to accurately predict the data, it did not account for the effects of other gas components, such as SO_2 and NO. Edwards *et al.* published a model that seemed to correspond well with experimental data (Edwards, Kilgroe & Srivastava, 2001). However, similar to Sliger and Widmer, several key constants were negative, and the inhibitory effect of SO_2 was not accounted for. Niksa *et al.* published a model to predict the importance of NO and H_2O in a gas stream (Fujiwara, Helble & Niksa, 2001). The predictions corresponded well with experimental data. However, the authors had to intentionally add oxygen radicals to their mechanism in order to initiate the reaction between elemental Hg and Cl radicals. Helble *et al.* developed a model using elemental reactions involving the impact of SO_2 on Hg oxidation (Helble *et al.*, 2003). Data was collected at temperatures above 1000 °C and the model provided accurate predictions. However, preliminary findings showed that the model was unable to predict data obtained in this work, and is perhaps not robust enough to predict a wide range of temperature data.

Table 1
Summary of Data from 11 Unique Sources (Data Includes Gas Composition, Chlorine Species Used, Gas Temperature Profile, Residence Time, Mercury Measurement Device, and Observed Percent Hg Oxidation.)

Author	Gas Composition								Oxidant		Temperature Range	Total Residence Time	Reactor Type	Hg Analyzer	Hg Oxidation
	N_2 (%)	O_2 (%)	CO_2 (%)	SO_2 (ppmv)	NO (ppmv)	CO (ppmv)	H_2O (%)	Hg (μg/m^3)	Cl_2 (ppmv)	HCl (ppmv)	(°C)	(seconds)		Type	(%)
Laudal[4]	71	4	15	0	0	0	10	20	10	0	175	1.00	Teflon	O-H Method[a]	84.8
				1500					0						0.7
				0						50					0.3
					600					0					2.1
									10	50					78.7
				1500					0						0.1
Norton[5]	82	6	12	1600	300	0	0	12	0	0	180	1.00	Stainless Steel	O-H Method[a]	0.0
				0						50					9.0
				1600	0										2.0
					300										5.0
Ghorishi[6]	93	2	5	0	0	0	0	40	0	200	754 - 25	0.97	Quartz	CEM[b]: Buck 400a	27.3
										100					15.5
										50					9.0
										200	634 - 25	1.00			18.3
										100					10.8
										50					5.8
										200	515 - 25	1.22			16.3
										100					9.0
										50					5.3
Kilgroe[7]	93	2	5	0	0	0	0	40	0	50	754 - 25	0.97	Quartz	CEM: Buck 400a	9.0
										100					16.0
										200					26.0
				500						50					3.5
										100					6.0
										200					17.5
	91.3						1.7			50					1.8
										100					8.0
										200					17.0
Mamani - Paco[8]	61	0	13	0	0	0	26	50	50	0	1080 - 25	1.40	Quartz	EPA Method 29 & CVAAS[c]	10.0
												6.20			7.0
												3.60			7.1
												1.40			12.0
									100			6.20			36.0
												1.40			45.0
									300			6.20			69.0
												1.40			66.0
									500			3.60			93.0
												6.20			92.0
												1.40			92.0
									0	100		1.40			2.0
												6.20			2.0
												3.60			2.0
									50			1.40			10.0
Qui[9]	71.2	2.8	0	0	0	0	26	50	250	0	1080 - 25	1.40	Quartz	EPA Method 29 & CVAAS	67.7
									500						94.5
				100					250						46.4
									500						77.4
				400					250						29.7
									500						62.4
				500					250						21.9
	73.4	0.6		0					250						61.0
									500						89.1
				100					250						27.3
									500						54.8
				500					250						10.4
Fry[10]	78.6	3.3	0	0	58	48	18.1	25	0^{++}	0	1130 - 175	6.00 Fast Quenching	Quartz	CEM: Tekran 2537A	0.0
										100					10.0
										200					15.6
										300					28.8
										400					66.2
										500					83.0
										600					86.1
										0					0.0
										100					10.0
										200					24.0
										300					39.2
										400					71.0
										500					83.0
										600					88.0
										0		6.00 Slow Quenching			0.0
										100					16.0
										200					64.2
										300					85.0
										400					91.0
										500					94.7
										600					96.0
										0					0.0
										100					29.2
										200					68.3
										300					85.0
										400					91.0
										500					96.7
										600					98.0

To be continued

Continued

Author	Gas Composition								Oxidant		Temperature Range (°C)	Total Residence Time (seconds)	Reactor Type	Hg Analyzer Type	Hg Oxidatio (%)
	N_2 (%)	O_2 (%)	CO_2 (%)	SO_2 (ppmv)	NO (ppmv)	CO (ppmv)	H_2O (%)	Hg (μg/m^3)	Cl_2 (ppmv)	HCl (ppmv)					
Hall[11]	90	10	0	0	500	0	0	150	0	12.5	500 - 25	1.40	Stainless Steel	CVAAS	8.0
										300					74.4
					0							1.00			88.5
										100		1.90			24.0
										200					26.0
									100	0		1.40			75.3
									150						78.5
Sliger[12-13]	74.12	7.43	6.15	0	25	0	12.3	100	0	56	997 - 25	1.40	Furnace lined with refractory material and/or Quartz	Simplified EPA Method 29	0.0
										172					33.0
										175					27.0
										282					41.0
										0	868 - 25				0.0
										0					2.0
										131					11.0
										0	1071 - 25				0.0
										638					75.0
	86.42						0			274	927 - 25				86.5
	81.42						5								79.5
	76.42						10								79.5
	72.42						14								75.5
															74.0
															71.5
Widmer[14]	72	10	10	0	0	0	8	3700	0	0	632 - 25	0.89	Quartz	EPA Method 29	0.0
										3000	631 - 25	0.89			80.0
											771 - 25	0.77			97.0
											876 - 25	0.70			95.0
										300	869 - 25	0.70			72.0
											649 - 25	0.87			22.0
											538 - 25	0.99			22.0
Agarwal[3, 15]	96.5	2.9	0	0	0	0	0	11.6	2	0	538 - 177	2.70	Stainless Steel	CEM: PSA	71.8
	83.5		13.5					13.4							76.9
	70			370	170	300	12.9	10.0							0.0
	83.5		0	0	0	0		10.5	27.5						89.5
	70		13.5					10.6							90.0
				370				10.3							56.9
					170			10.6							45.7
						300		10.8							44.4
	83.5		0	0	0	0		10.5	27.5						94.6
	70		13.5					10.6							93.2
				370				10.3							66.6
					170			10.6							51.4
						300		10.8							53.7
	100	0	0	0	0	0	0	1.1	1.0		166 - 121	3.27			73.1
								1.2			347 - 121	2.96			52.7
								10.9			169 - 121	3.27			69.2
								11.7			353 - 121	2.96			53.5
								11.6			582 - 121	2.70			49.4
								10.9			232 - 121	3.10			70.1
								11.6	5.0		232 - 121	3.10			91.6
								14.7			385 - 121	2.96			89.2
								11.2			593 - 121	2.70			97.8
	87	0	0	0	0	0	13	12.7	12.4		320 - 163	2.96			71.1
									30.9						87.4
									51.8						93.7
								11.7	11.6		430 - 163	2.84			80.9
									30.5						90.3
									51.8						94.6

[a] O-H Method – Ontario-Hydro Method
[b] CEM – Continuous Emissions Monitor
[c] CVAAS – Cold Vapor Atomic Adsorption Spectroscopy
[++] ‘0’ for Cl_2 is explained by Fry et al. by way of complete dissociation of the molecule to Cl ions and thereby giving an equivalent for HCl. So for example, 50 ppm Cl_2 gives an equivalent of 100 ppm HCl.

In summary, temperature plays an important role in Hg oxidation. HCl is important in oxidizing Hg at higher temperatures (above approximately 700 °C), while Cl_2 oxidizes Hg at lower temperatures (below 700 °C). It has also been reported that NO, SO_2 and H_2O inhibit the oxidation of Hg by either chlorine species (Cl_2 or HCl). Due to the wide variety of published experimental data, the development of a global kinetic model is important and would be best suited to accurately predict the speciation of Hg. All the experimental data used in this model is summarized in Table 1. This paper introduces such a model, where five global reactions are used. These reactions are:

$$Hg(g)+Cl_2(g)\overset{k_1}{\longleftrightarrow}HgCl_2(g) \tag{1}$$

$$H_2O(g)+Cl_2(g)\overset{k_2}{\longleftrightarrow}2HCl(g)+\tfrac{1}{2}O_2(g) \tag{2}$$

$$Hg(g)+2HCl(g)\xrightarrow{k_3}HgCl_2(g)+H_2(g) \tag{3}$$

$$HgCl_2(g)+SO_2(g)\xrightarrow{k_4}Hg(g)+SCl_2(s,g)+O_2(g) \tag{4}$$

$$2NO(g)+Cl_2(g)\xrightarrow{k_5}2NOCl(g) \tag{5}$$

Reactions 1 and 2 are reversible, while reactions 3, 4 and 5 are irreversible. The 'k' terms are the reaction rate constants for each reaction.

3. TESTING FACILITY

The proposed global reaction scheme was formulated from data obtained in a testing facility that was described in greater detail in an earlier publication (Agarwal *et al.*, 2006). Figure 1 shows a schematic of the testing facility built to perform Hg oxidation tests. The various gas components were metered, blended and heated to the desired temperature. The bulk gas stream (consisting of N_2, O_2 and CO_2) was preheated in the air pre-heater (APH) to temperatures between 100 and 320 °C. The steam pre-heater (SPH) was used to vaporize liquid water to superheated steam at temperatures between 100 and 300 °C. The bulk gases, trace gases (consisting of SO_2, NO and CO) and steam were heated and mixed in the final pre-heater (R1). The gas mixture temperature at the exit of R1 ranged between 166 to 570 °C. These temperatures were chosen due to the lack of published Hg data and because the thermodynamic transition from Hg to $HgCl_2$ occurs in this range.

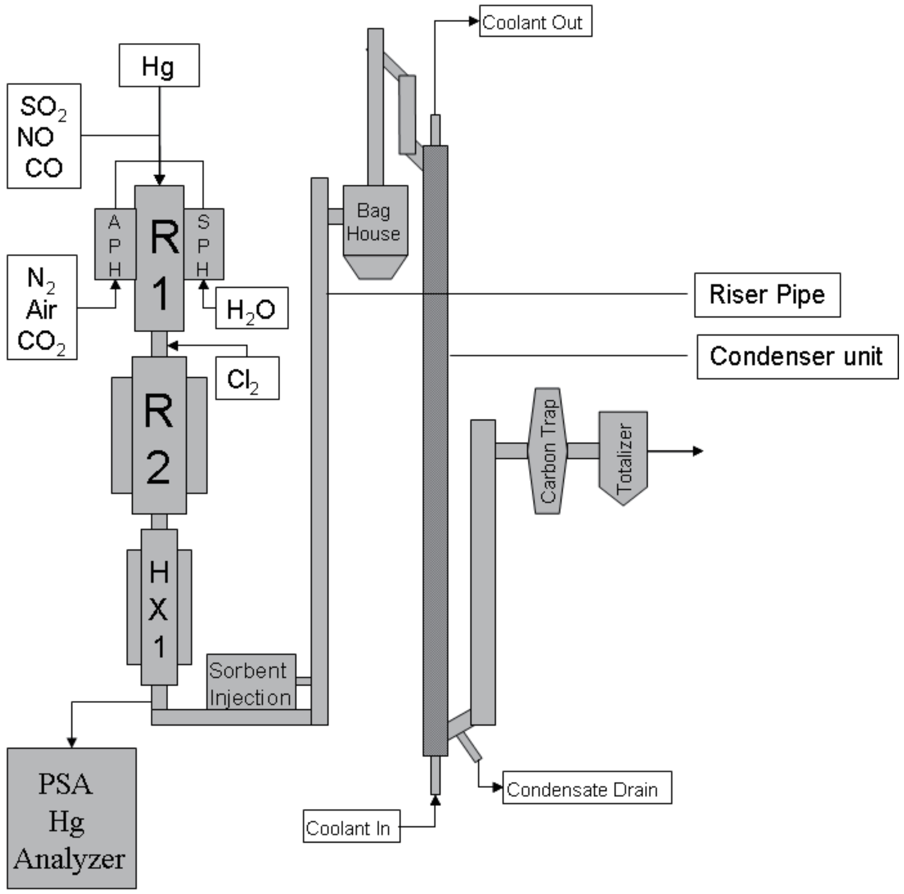

Figure 1
Schematic of Testing Facility Used to Perform Hg Oxidation Tests

The oxidant used was chlorine gas (Cl_2) and was injected as a one percent mixture in N_2 at the entrance of R2. R2 is a 4 in. ID, 36 in. long Inconel pipe and provided a residence time between 1.7 and 2.2 seconds. Mercury oxidation took place within R2, and the gas stream was cooled through a controllable temperature profile. A third section of the apparatus, labeled HX1, provided additional residence time and further cooled the gas stream. A ¼ in. port at the exit of R2 and HX was available for gas sampling. The sample gas was transported at a rate of 6 liters per minute (LPM) via a heated Teflon line at approximately 150 °C. The calculated residence time of the gas stream in the sample line was less than 0.1 seconds.

A PS Analytical Sir Galahad 10.525 semi-continuous Emissions Monitoring system (SCEM) was used to measure elemental and total Hg in the gas stream. Table 1 summarizes the collected data.

4. NUMERICAL MODEL

An introduction to the reactions used in the global kinetic model used in this work is given in prior publications (Agarwal *et al.*, 2003, 2007). As mentioned earlier, five global reactions are proposed for this model, two reversible and three irreversible. Reaction 1 is the global mercury oxidation reaction, where elemental Hg reacts with Cl_2 to form $HgCl_2$. Reaction 2 is the Deacon reaction. This reaction was chosen because at high Cl_2 concentrations, it is kinetically favored in the forward direction and water consumes Cl_2 to form HCl. This would result in less Cl_2 remaining to oxidize elemental Hg at lower temperatures. Since HCl is formed by the Deacon Reaction, Reaction 3 was chosen to account for the reaction between Hg and HCl at high temperatures to form $HgCl_2$ and H_2. Reaction 4 accounts for the inhibitory effect of SO_2 by reducing $HgCl_2$ to elemental Hg. Reaction 5 was proposed in a prior publication and accounts for the inhibitory effect of NO on the oxidation of Hg by Cl_2 since NO reacts with Cl_2 to form NOCl (Agarwal *et al.*, 2006). These reactions are shown to support the observed trends of Cl_2 concentration, temperature, water and SO_2 and NO addition, as obtained in the experiments described in a previous section. The reactor model used is a non-isothermal plug flow reactor (PFR) system.

At atmospheric pressure, the reaction rates for the reactions can be written as:

$$r_1 = k_1 \cdot \left(y_{Hg} \cdot y_{Cl_2} - \frac{y_{HgCl_2}}{Keq_1} \right) \tag{6}$$

$$r_2 = k_2 \cdot \left(y_{H_2O} \cdot y_{Cl_2} - \frac{y_{HCl}{}^2 \cdot y_{O_2}{}^{1/2}}{Keq_2} \right) \tag{7}$$

$$r_3 = k_3 \cdot \left(y_{Hg} \cdot y_{HCl}{}^2 \right) \tag{8}$$

$$r_4 = k_4 \cdot \left(y_{HgCl_2} \cdot y_{SO_2} \right) \tag{9}$$

$$r_5 = k_5 \cdot \left(y_{Cl_2} \cdot y_{NO}{}^2 \right) \tag{10}$$

Each y term in Equations 6 to 10, except for H_2O and O_2, represents the concentration of each species in ppm. In the case of H_2O and O_2 the respective concentrations are in mole fraction. The rate constants, k_1 to k_5 are temperature dependent and are defined by Equation 11:

$$k = A \cdot \exp[\frac{-E}{R \cdot T}] \tag{11}$$

Where A is the pre-exponential factor, E is the activation energy (in kcal/mole), R is the universal gas constant (1.987 cal/mole/K), and T is the temperature in degrees Kelvin. Typically, the Arrhenius equation includes a third term (T^n). The value of 'n' was set to zero for all reactions to simplify the kinetic mechanism.

Since Reactions 1 and 2 are reversible, the rates of these reactions are dependent on the equilibrium constants, which are a function of temperature. A simple equilibrium calculation using the RGIBBS reactor model in the software Aspen Plus was done to find this temperature dependence (Agarwal *et al.*, 2007). The reaction rates for each of the reactions can, therefore, be written as:

$$r_1 = A_1 \cdot \exp[\frac{-E_1}{R \cdot T}] \cdot \left([Hg] \cdot [Cl_2] - \frac{[HgCl_2]}{\exp\left[-17.833 + \frac{17133.1}{T}\right]} \right) \tag{12}$$

$$r_2 = A_2 \cdot \exp[\frac{-E_2}{R \cdot T}] \cdot \left([H_2O] \cdot [Cl_2] - \frac{[HCl]^2 \cdot [O_2]^{1/2}}{\exp\left[13.707 - \frac{4769.2}{T}\right]} \right) \tag{13}$$

$$r_3 = A_3 \cdot \exp[\frac{-E_3}{R \cdot T}] \cdot [Hg] \cdot [HCl]^2 \tag{14}$$

$$r_4 = A_4 \cdot \exp[\frac{-E_4}{R \cdot T}] \cdot [HgCl_2] \cdot [SO_2] \tag{15}$$

$$r_5 = A_5 \cdot \exp[\frac{-E_5}{R \cdot T}] \cdot [NO]^2 \cdot [Cl_2] \tag{16}$$

The concentrations of the pertinent species as a function of residence time are shown in Equations 17 to 20. The term, *t*, is the residence time in the reactor system, and the concentrations ([*Hg*]) are in ppm. Since the concentrations of O_2 and H_2O are several orders of magnitude higher than the concentrations of the other species, their rates of change are insignificant.

$$R_{Hg} = \frac{d[Hg]}{dt} = r_4 - r_1 - r_3 \tag{17}$$

$$R_{HgCl_2} = \frac{d[HgCl_2]}{dt} = r_1 + r_3 - r_4 \tag{18}$$

$$R_{Cl_2} = \frac{d[Cl_2]}{dt} = -r_1 - r_2 - r_5 \tag{19}$$

$$R_{HCl} = \frac{d[HCl]}{dt} = r_2 - r_3 \tag{20}$$

Equations 17 to 20 were solved numerically using a fourth order Runge Kutta routine (Matlab function: ODE45). This function is a computing one-step solver for which it needs only the solution at the immediately preceding time point. In order to optimize the fit between experimentally measured Hg conversions and the model predictions, a simplex routine (Matlab function: fminsearch) was used to minimize the function shown in Equation 21:

$$ERROR = \sum_{i=1}^{N} (x_{Hg,\text{model}} - x_{Hg,\text{data}})_i^2 \tag{21}$$

where *x* is the conversion of elemental mercury to the oxidized form.

The pre-exponential factors (A_1, A_2, A_3, A_4, A_5) and activation energies (E_1, E_2, E_3, E_4, E_5) for the five respective reactions were varied in order to minimize the function in Equation 21.

5. RESULTS AND DISCUSSION

The values of A and E were determined for the five reactions in the global kinetic model. The effectiveness of the proposed scheme was shown by plotting the observed experimental values on the y-axis and the predicted values on the x-axis from the published experimental data. Ideally, all the data points should lie on the y = x line (shown as the dashed line), which would imply that the fit was perfect.

Initially, only Reaction 1 was used to predict the data. Figure 2 shows the observed versus the predicted percent Hg oxidation. The values for A and E are shown in the insert. As expected, this reaction alone is insufficient to accurately predict the data. Most of the predicted data is clustered around the axes. The calculated average error is 33.86.

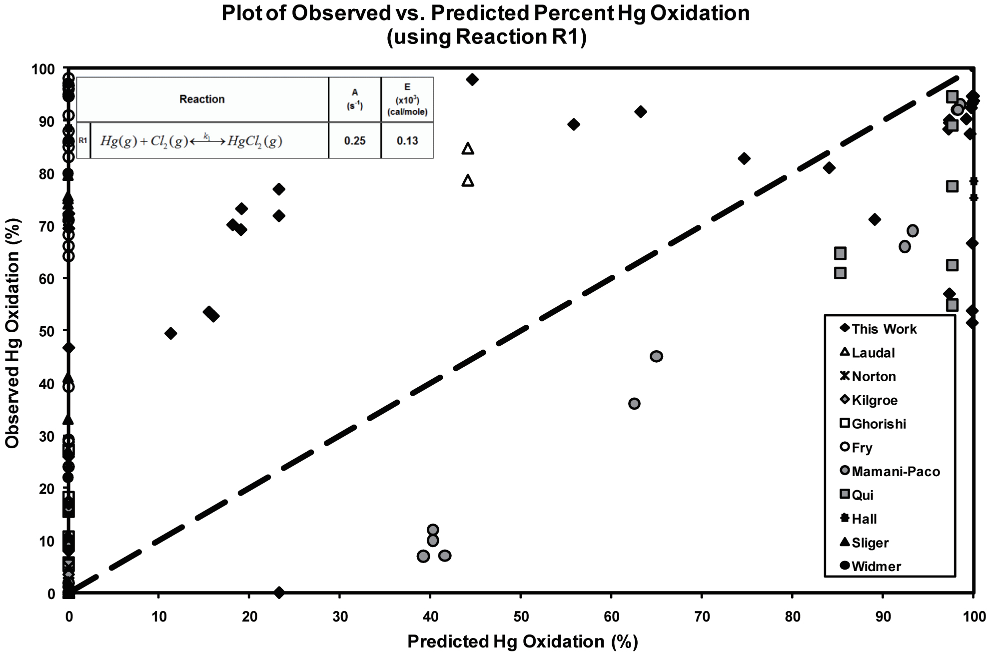

Figure 2
Plot of Observed Hg Oxidation Versus Predicted Hg Oxidation, Using Reaction 1

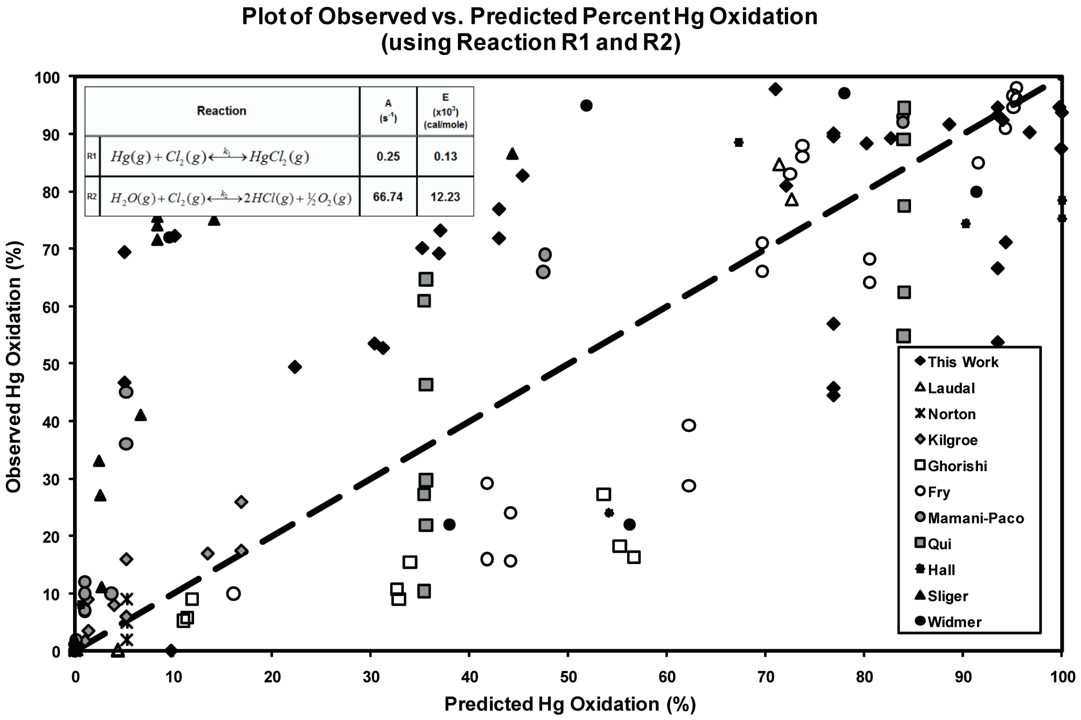

Figure 3
Plot of Observed Hg Oxidation Versus Predicted Hg Oxidation, Using Reactions 1 and 2

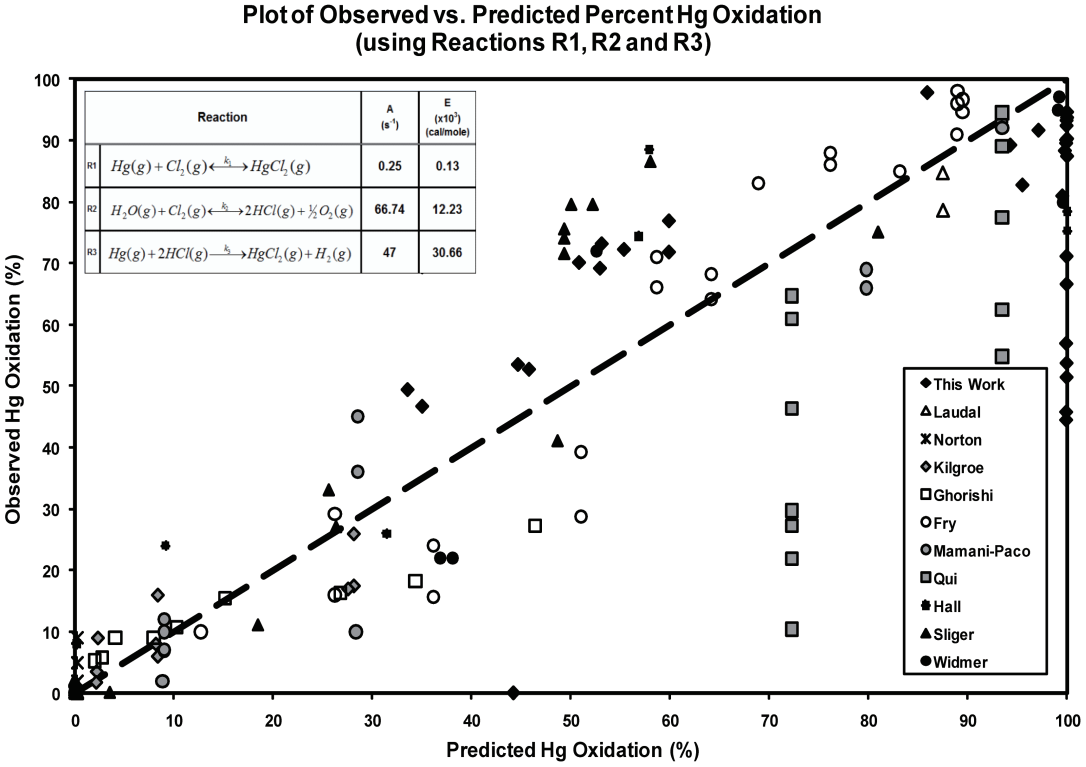

Figure 4
Plot of Observed Hg Oxidation Versus Predicted Hg Oxidation, Using Reactions 1, 2 and 3

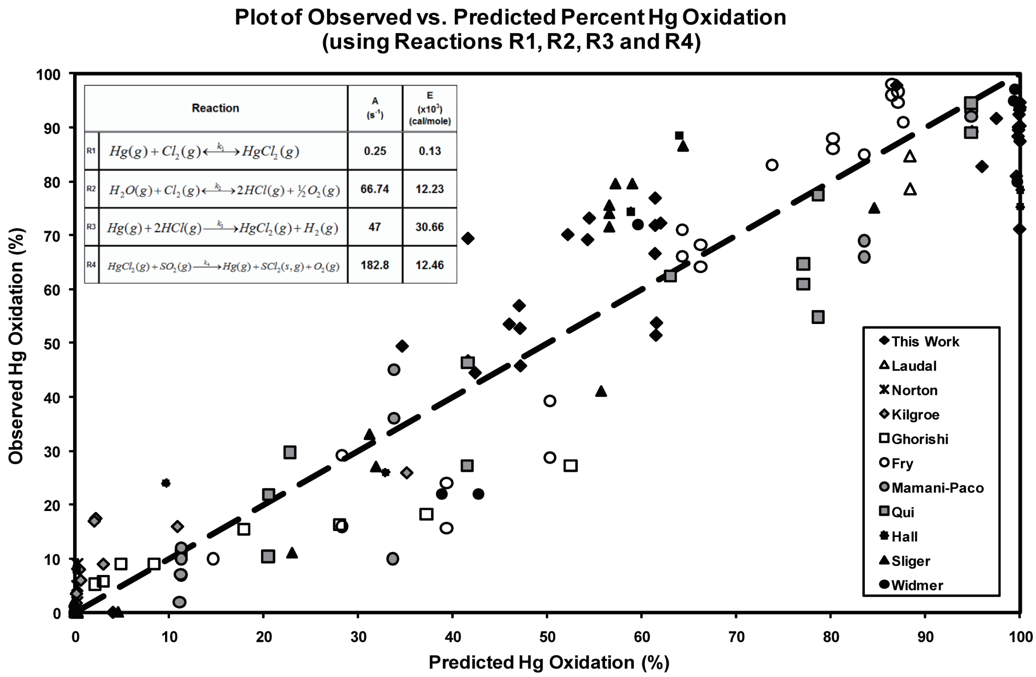

Figure 5
Plot of Observed Hg Oxidation Versus Predicted Hg Oxidation, Using Reactions 1, 2, 3 and 4

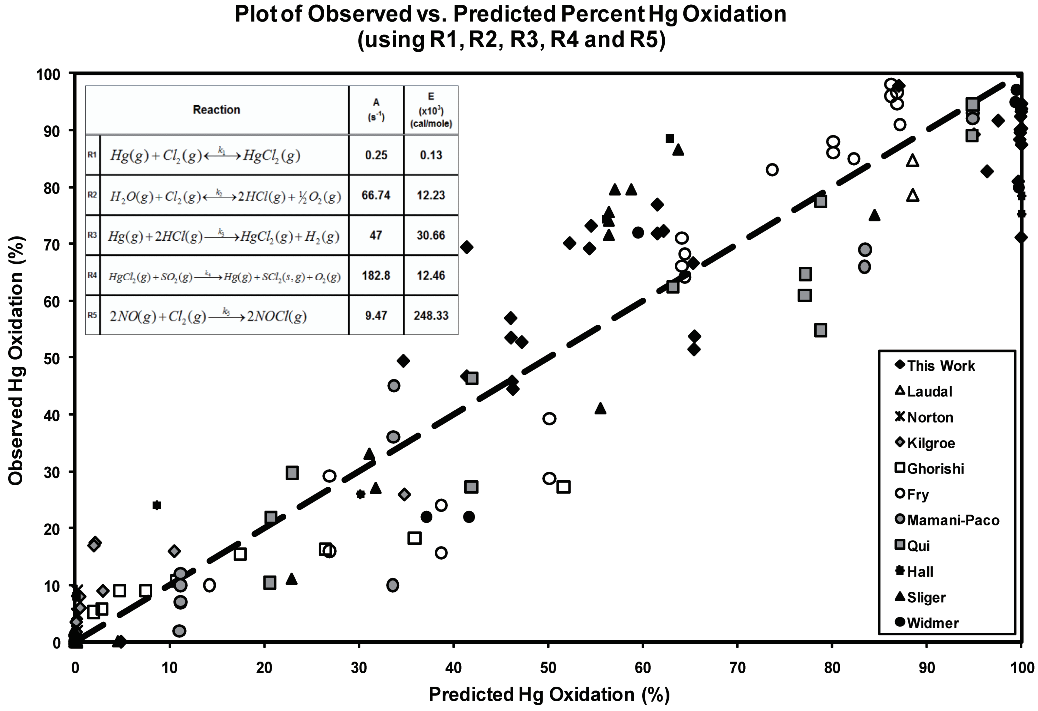

Figure 6
Plot of Observed Hg Oxidation Versus Predicted Hg Oxidation, Using Reactions 1, 2, 3, 4 and 5

Reaction 2 (Deacon Reaction) was then added to the model. It is known that the Deacon Reaction is initiated by a catalyst (Deacon). Since the experiments in previous publications were carried out in a stainless steel and Inconel pipe, and Inconel is known to contain iron and traces of manganese, silicon and aluminum (Magellan Metals, 2012), the oxides of these metals are potential catalysts for the reaction to proceed (Deacon and Edwards). The result of adding this reaction to the model is shown in Figure 3 along with the values of A and E. The data is still scattered, the calculated average error improved to 17.65.

As determined by other researchers, HCl is an effective oxidizing agent at high temperatures. Reaction 3 takes this into account. The reaction was added to the model and the results are shown in Figure 4. The values of A and E for the 3 reactions (R1, R2 and R3) are shown. The calculated average error improved to 12.49.

There is limited published information regarding the inhibitory effect of molecular SO_2 on the oxidation of Hg by a chlorine species. Qiu *et al.* suggested this inhibitory effect and proposed two reactions involving SO and SCl (Helble, 2003). They stated that these radicals scavenge chlorine radicals, which may be present at higher temperatures. It is postulated that the chlorine radical is important for the initial oxidation reaction that converts elemental Hg to HgCl (Fujiwara, 2001). Reaction 4 is a new reaction that is proposed in this paper. This reaction does not involve radicals, and instead reduces $HgCl_2$ in the gas phase to elemental Hg, SCl_2 and O_2. Figure 5 shows the result of adding this reaction to the model and the calculated error is reduced to 8.77.

Reaction 5 was proposed in a previous publication to take into account any inhibitory effect of NO on Hg oxidation by Cl_2 (Agarwal *et al.*, 2006). The fit (shown in Figure 6) was not affected significantly. The distribution of the data points and the calculated error between Figures 5 and 6 are almost identical. Regardless, this reaction was included in the model for completeness. Table 2 shows the final values of A and E for the 5 reactions as used in the model.

Table 2
Summary of the Values for the Pre-Exponential Factor (A) and Activation Energy (E) for Each of the Reactions Used in this Model

	Reaction	A (s^{-1})	E ($\times 10^3$) (cal/mole)	$k = A \cdot \exp[\frac{-E}{R \cdot T}]$
1	$Hg(g) + Cl_2(g) \xleftrightarrow{k_1} HgCl_2(g)$	0.25	0.13	$k_1 = 0.25 \cdot \exp[\frac{-0.13 \times 10^3}{1.987 \cdot T}]$
2	$H_2O(g) + Cl_2(g) \xleftrightarrow{k_2} 2HCl(g) + \frac{1}{2}O_2(g)$	66.74	12.23	$k_2 = 66.74 \cdot \exp[\frac{-12.23 \times 10^3}{1.987 \cdot T}]$
3	$Hg(g) + 2HCl(g) \xrightarrow{k_3} HgCl_2(g) + H_2(g)$	47.00	30.66	$k_3 = 47.00 \cdot \exp[\frac{-30.66 \times 10^3}{1.987 \cdot T}]$
4	$HgCl_2(g) + SO_2(g) \xrightarrow{k_4} Hg(g) + SCl_2(s,g) + O_2(g)$	182.80	12.46	$k_4 = 182.80 \cdot \exp[\frac{-12.46 \times 10^3}{1.987 \cdot T}]$
5	$2NO(g) + Cl_2(g) \xrightarrow{k_5} 2NOCl(g)$	9.47	248.33	$k_5 = 9.47 \cdot \exp[\frac{-248.33 \times 10^3}{1.987 \cdot T}]$

Experimental data collected by individual research groups was used to validate the model proposed in this paper. Each figure shows the predicted versus observed values, and as expected, some data fits better than others. Table 3 shows the numerical results from the model. The variation between predicted and observed percent Hg oxidation does not exceed 30 percent for any of the data points. This is significant, considering the large range of experiments included in the validation.

As is the case for any effort to correlate observed and predicted data, there are certain limitations of this global predictive model:

(1) The Arrhenius Equation typically includes a temperature dependent term (T^n), where "n" is a constant. In order to simplify this model, the effect of this term was assumed to be insignificant, and "n" was set to zero.

(2) In addition to the bulk and trace gases mentioned earlier, typical flue gas also consists of carbon monoxide (CO) and hydrogen sulfide (H_2S). These components were not included in the model since there is limited to no published data on the effects on homogeneous oxidation of Hg.

(3) Many coal-fired power plants are required to control NOx emissions, and do so by injecting ammonia (NH_3) into the boiler back-end. The combination of NH_3 in the gas stream and a reduced NO concentration may affect the oxidation of Hg. However, it is unclear to what extent.

(4) In addition to controlling NO_x, power plants are required to control the inadvertent conversion of SO_2 to SO_3. It is unclear if SO_3 in the flue gas affects the oxidation of Hg in any way.

(5) Coal-fired power plants typically have ESP or a bag-house to trap particulate mercury (Hg^P). It is likely that the presence of unburnt carbon and fly ash in the flue gas results in heterogeneous Hg oxidation, or the formation of Hg^P. However, the extent of this conversion is unclear and needs to be studied further. This is especially difficult since the amount of unburnt carbon and fly ash composition differs based on the boiler efficiency and the coal that is burnt in the boiler.

Table 3
Numerical Results Comparing the Observed Percent Hg Oxidation (with Corresponding Researcher) Versus the Predicted Percent Hg Oxidation from the Model

	Observed Hg Oxidation (%)	Predicted Hg Oxidation (%)	Absolute % Difference
Laudal[4]	84.8	88.49	3.7
	0.7	0.00	0.7
	0.3	0.18	0.1
	2.1	0.00	2.1
	78.7	88.51	9.8
	0.1	0.17	0.1
Norton[5]	0.0	0.00	0.0
	9.0	0.23	8.8
	2.0	0.21	1.8
	5.0	0.21	4.8
Ghorishi[6]	27.3	51.63	24.3
	15.5	17.47	2.0
	9.0	4.73	4.3
	18.3	35.90	17.6
	10.8	10.75	0.0
	5.8	2.85	2.9
	16.3	26.47	10.2
	9.0	7.53	1.5
	5.3	1.98	3.3
Kilgroe[7]	9.0	2.96	6.0
	16.0	10.50	5.5
	26.0	34.79	8.8
	3.5	0.14	3.4
	6.0	0.56	5.4
	17.5	2.14	15.4
	1.8	0.13	1.6
	8.0	0.51	7.5
	17.0	2.01	15.0
Mamani - Paco[8]	10.0	11.19	1.2
	7.0	11.18	4.2
	7.1	11.17	4.1
	12.0	11.19	0.8
	36.0	33.66	2.3
	45.0	33.73	11.3
	69.0	83.46	14.5
	66.0	83.42	17.4
	93.0	94.81	1.8
	92.0	94.78	2.8
	92.0	94.83	2.8
	2.0	11.07	9.1
	2.0	11.05	9.1
	2.0	11.05	9.1
	10.0	33.59	23.6
Qui[9]	67.7	77.12	9.4
	94.5	94.83	0.3
	46.4	41.93	4.5
	77.4	78.79	1.4
	29.7	22.95	6.7
	62.4	63.19	0.8
	21.9	20.69	1.2
	61.0	77.11	16.1
	89.1	94.79	5.7
	27.3	41.90	14.6
	54.8	78.78	24.0
	10.4	20.62	10.2
Fry[10]	0.0	0.00	0.0
	10.0	14.27	4.3
	15.6	38.73	23.1
	28.8	50.13	21.3
	66.2	64.12	2.0
	83.0	73.64	9.4
	86.1	80.10	6.0
	0.0	0.00	0.0
	10.0	14.27	4.3
	24.0	38.73	14.7
	39.2	50.13	10.9
	71.0	64.12	6.8
	83.0	73.64	9.4
	88.0	80.10	7.9
	0.0	0.00	0.0
	16.0	26.91	10.9
	64.2	64.45	0.3
	85.0	82.29	2.7
	91.0	87.14	3.9
	94.7	86.85	7.9
	96.0	86.19	9.8
	0.0	0.00	0.0
	29.2	26.91	2.3
	68.3	64.45	3.8
	85.0	82.29	2.7
	91.0	87.14	3.9
	96.7	86.85	9.9
	98.0	86.19	11.8
Hall[11]	8.0	0.15	7.8
	74.4	56.15	18.2
	88.5	62.85	25.6
	24.0	8.68	15.3
	26.0	30.21	4.2
	75.3	100.00	24.7
	78.5	100.00	21.5
Sliger[12-13]	0.0	4.61	4.6
	33.0	31.14	1.9
	27.0	31.81	4.8
	41.0	55.52	14.5
	0.0	0.00	0.0
	2.0	0.00	2.0
	11.0	22.94	11.9
	0.0	0.00	0.0
	75.0	84.43	9.4
	86.5	63.73	22.8
	79.5	58.77	20.7
	79.5	57.04	22.5
	75.5	56.41	19.1
	74.0	56.41	17.6
	71.5	56.41	15.1
Widmer[14]	0.0	0.00	0.0
	80.0	99.63	19.6
	97.0	99.40	2.4
	95.0	99.29	4.3
	72.0	59.48	12.5
	22.0	41.68	19.7
	22.0	37.12	15.1
Agarwal[3, 15]	71.8	61.55	10.3
	76.9	61.55	15.4
	0.0	4.94	4.9
	89.5	99.87	10.4
	90.0	99.87	9.9
	56.9	46.07	10.8
	45.7	46.21	0.5
	44.4	46.31	1.9
	94.6	99.97	5.4
	93.2	99.97	6.7
	66.6	65.33	1.2
	51.4	65.42	14.0
	53.7	65.48	11.8
	73.1	54.57	18.6
	52.7	47.24	5.5
	69.2	54.39	14.8
	53.5	46.11	7.4
	49.4	34.75	14.7
	70.1	52.30	17.8
	91.6	97.531	5.9
	89.2	94.984	5.8
	97.8	87.048	10.8
	71.1	99.96	28.9
	87.4	100.00	12.6
	93.7	100.00	6.3
	80.9	99.65	18.7
	90.3	99.81	9.6
	94.6	99.90	5.3

CONCLUSIONS AND FURTHER WORK

A global kinetic model was developed to predict Hg oxidation by chlorine species. Five reactions were proposed to predict published experimental data produced using simulated flue gas containing Hg. Two of the five reactions are reversible, the remaining three were irreversible. Eleven independent researchers' data, consisting of a number of variables, were used to validate the model. This contributes to the robustness of the model. The following features can be obtained from the model:

(1) The oxidation of Hg by Cl_2 -- where the concentration of Cl_2 ranges from 1 to 500 ppm_v.

(2) The oxidation of Hg by HCl -- where the concentration of HCl ranges from 50 to 3000 ppm_v.

(3) The effect of a wide range of temperatures -- from 175 °C to over 1100 °C.

(4) The effect of a wide range of residence times -ranging from 0.70 seconds to 6.2 seconds.

(5) The inhibitory effect of SO_2 on Hg oxidation by a chlorine species -- where the concentration of SO_2 ranged from 100 ppm_v to 1600 ppm_v.

(6) The use of different reactor types -- Teflon, Quartz, a furnace lined with refractory material, and stainless steel.

(7) The use of different methods of measuring the mercury species -- the most commonly used methods were the Ontario-Hydro Method and a Continuous Emissions Monitoring (CEM) device. The EPA Method 29 and cold vapor atomic adsorption spectroscopy (CVAAS) were also used.

The global scheme was able to predict the data from up to eleven experimental data sources. Of the eleven data sources, 140 data points were used to validate the global scheme, and nearly 90% of these data points were accurately predicted.

Further work for this model would involve the addition of the temperature dependent term (T^n) in the Arrhenius equation. In addition, a sensitivity analysis should be done to predict trends of Hg oxidation for each of the flue gas components.

REFERENCES

[1] U.S. Environmental Protection Agency, Office of Air Quality Planning and Standards and Office of Research and Development. (1997). *Mercury Study Report to Congress: Executive Summary* (Vol. I). Report No. EPA-452/R-97-003. Washington, DC: U.S. Environmental Protection Agency.

[2] Brown, Hargis, Smith, D.N., & O'Dowd, W.J. (1999). Mercury Measurement and Its Control: What We Know, have Learned, and Need to Further Investigate. *Journal of Air and Waste Management Association, 49,* 1-97.

[3] Agarwal, Romero, C.E., & Stenger, H.G. (2007). Comparing and Interpreting Laboratory Results of Hg Oxidation by a Chlorine Species. *Fuel Process Technology*, *88*, 723-730.

[4] Brown, Laudal, D.L., & Nott, B.R. (2000). Effects of Flue Gas Constituents on Mercury Speciation. *Fuel Process Technology*, *65-66*, 157-165.

[5] Brown, Dunham, Eryavec, Laudal, Norton, G.A., & Yang, H. (2002). Heterogeneous Oxidation of Mercury in Simulated Post Combustion Conditions. *Fuel*, *82*, 107-116.

[6] Ghorishi, S.B. (1998). *Fundamentals of Mercury Speciation and Control in Coal-Fired Boilers* (Report EPA-600/R-98-014). Washington, DC: U.S. Environmental Protection Agency.

[7] Kilgroe, J.D., Lee, C.W., Ryan, J.V., Sedman, C.B., Srivastava, R.K., & Thorneloe, S.A. (2001). *Control of Mercury Emissions from Coal-Fired Electric Utility Boilers* (Interim Report, No. EPA-600/R-01-109). Washington DC: U.S. Environmental Protection Agency.

[8] Helble, J.J., & Mamani-Paco, R.M. (Eds.). (2000). *Bench-Scale Examination of Mercury Oxidation Under Non-Isothermal Conditions: Proc. A&WMA Annual Conference*. Salt Lake City, UT.

[9] Helble, J.J., Qiu, J., & Sterling, R.O. (Eds.). (2003). *Development of an Improved Model for Determining the Effects of SO_2 on Homogeneous Mercury Oxidation: Clear Water Conference*. Clearwater, FL.

[10] Cauch, B., Fry, A., Lighty, J.S., Senior, C.L., & Silcox, G.D. (Eds.). (2005). *Detailed Kinetic Modeling of Homogeneous Mercury Oxidation Reactions in a 1000 Btu/hr Quartz Furnace: 22nd International Pittsburgh Coal Conference*. Pittsburgh, PA.

[11] Hall, Lindqvist, O., & Schager, P. (1991). Chemical Reactions of Mercury in Combustion Flue Gases. *Water, Air, Soil Pollut, 56*, 3-14.

[12] Kramlich, Marinov, N.M., & Sliger, R.N. (2000). Towards the Development of a Chemical Kinetic Model for the Homogenous Oxidation of Mercury by Chlorine Species. *Fuel Process Technology*, *65-66*, 423-438.

[13] Sliger, R.N. (2001). *Development of a Chemical Kinetic Model for the Homogeneous Oxidation of Mercury by Chlorine Species: A Tool for Mercury Emissions Control* (Unpublished doctoral dissertation). University of Washington, USA.

[14] Cole, Gaspar, Seeker, W.R., & Widmer, N.C. (1998). Practical Limitation of Mercury Speciation in Simulated Municipal Waste Incinerator Flue Gas. *Combustion Science and Technology*, *134*, 315-326.

[15] Agarwal, Fan, Stenger, H.G., & Wu, S. (2006). The Effects of H_2O, SO_2 and NO on Homogeneous Hg Oxidation by Cl_2. *Energy and Fuel*, *20*, 1068-1075.

[16] Liu, J. (Ed.). (2008). *Modeling of Homogeneous Mercury Oxidation in Flue Gas during Coal Combustion: The 42nd Western Regional Meeting*. Las Vegas, NV.

[17] Xu, M. (2003). Modeling of Homogeneous Mercury Speciation Using Detailed Chemical Kinetics. *Combustion and Flame*, *132*, 208-218.

[18] Cole, J.A., West, J., & Widmer, N.C. (Eds.). (2000). *Thermochemical Study of Mercury Oxidation in Utility Boiler Flue Gases: Proceedings of the Air and Waste Management Association's 93rd Annual Meeting*. Salt Lake City, UT.

[19] Edwards, Kilgroe, J.D., & Srivastava, R.K. (2001) A Study of Gas-Phase Mercury Speciation Using Detailed Chemical Kinetics. *Journal of Air & Waste Management Association*, *51*, 869–877.

[20] Agarwal, H., & Stenger, H.G. (2007). Development of a Predictive Kinetic Model for Homogeneous Hg Oxidation Data. *Mathematical and Computer Modeling, 45*, 109-125.

[21] Magellan Metals. (2012). *Inconel 625*. Retrieved from http://www.magellanmetals.com/inconel_625.html

[22] Deacon, H. (1875). *Improvement in Manufacture of Chlorine. Patent No. 165802*. United States Patent and Trademark Office.

[23] Edwards, J.R., Ghorishi, S.B., Kilgroe, J.D., Lee, C.W., & Srivastava, R.K. (Eds.). (2001). *A Computational and Experimental Study of Mercury Speciation as Facilitated by the Deacon Process: The A&WMA Specialty Conference on Mercury Emissions: Fate, Effects and Control*. Chicago, IL.

[24] Fujiwara, Helble, J.J., & Niksa, S. (2001). Kinetic Modeling of Homogeneous Mercury Oxidation: The Importance of NO and H_2O in Predicting Oxidation in Coal-Derived Systems. *Environ. Sci. Technology, 35*, 3701-3706.